ARTICLE IN PRESS

Surface & Coatings Technology xxx (xxxx) xxx–xxx

Contents lists available at ScienceDirect

Surface & Coatings Technology

journal homepage: www.elsevier.com/locate/surfcoat

Laser cladding Ni-based alloy/nano-Ni encapsulated h-BN self-lubricating composite coatings

Hua Yan[a,b,*], Peilei Zhang[a,b], Qiushi Gao[a], Yang Qin[a], Ruidi Li[c]

[a] School of Materials Engineering, Shanghai University of Engineering Science, Shanghai 201620, China
[b] R & D Center for Key Technologies of Intelligent Ultra-intense Laser Processing Equipment, Shanghai 201620, China
[c] State Key Laboratory of Powder Metallurgy, Central South University, Changsha 410083, China

ARTICLE INFO

Keywords:
Laser cladding
Microstructure
Nano-Ni encapsulated h-BN
Self-lubricating coatings

ABSTRACT

Nano-Ni encapsulated h-BN/Ni-based alloy (Ni60) self-lubricating composite coatings on a medium carbon steel were fabricated by laser cladding using two types of lasers: a 5 kW continuous wave (CW) CO_2 laser and a 400 W pulsed Nd:YAG laser, respectively. A high-energy ball milling method was adopted to clad nano-Ni onto nano-h-BN with an aim to enhance the compatibility between the h-BN and the metal matrix during laser cladding processing. The microstructure, phase structure and wear properties of the self-lubricating composite coatings were investigated by means of scanning electron microscopy (SEM) and X-ray diffraction (XRD), as well as dry sliding wear testing. The research indicated that laser cladding of the self-lubricating composite coatings demonstrates sound cladding layers free of cracks and porosities. It was found that a reaction between h-BN and Ni-based alloy occurred, which generated hard phase CrB and Ni_3B leading to the increasing of the microhardness of the coatings by CO_2 laser cladding, while laser molten pool suppressed h-BN floating up to upper regions of coating for lower temperature and rapid solidification by YAG laser cladding. The high energy ball milling of nano-Ni onto nano-h-BN significantly improved the interfacial compatibility between h-BN and Ni60 matrix. The friction coefficient of the laser-clad Ni60/nano-Ni encapsulated h-BN coating was reduced obviously.

1. Introduction

Metal matrix lubricating composites combining both good wear resistance/toughness of metal matrix and excellent lubricating characteristic of lubricants, exhibit excellent tribological characteristics and good suitability to different atmospheric, chemical, electric and thermometric environments [1–3]. Cu-, Ag-, Ni-based alloys composites are extensively used in friction devices of various machines and mechanisms because of good heat conductivity, wear resistance, and stable chemical properties. Solid lubricants, such as graphite, metal sulfides (WS_2, MoS_2, MnS), hexagonal BN, CaF_2 etc., can be added into Cu (Ag, Ni) matrix for improving wear resistance [4–9].

Hexagonal boron nitride (h-BN) has a lamellar crystalline structure which is similar to those of graphite and molybdenum disulfide (MoS_2). This kind of structural properties of h-BN could be easily sheared along the basal plane of the h-BN and used as solid lubricant additives. Metal matrix h-BN lubricant composites are generally utilized in a form of coating or film instead of bulk composite because friction/wear always takes place on work piece surfaces. It has been used in different anti-wear applications. Several surface coating techniques such as thermal spraying [10–13], electroless plating [14,15], and laser cladding [16–19] have been reported for producing metal matrix h-BN composite coatings. I. Ozdemir et al. reported that FeB/h-BN coatings [11] and Al-12Si/TiB_2/h-BN composite [12] were deposited onto an aluminum substrate by atmospheric DC plasma spraying to improve its tribological properties. O.A. Leon et al. [14,15] reported that Ni-P-BN(h) coatings with thickness ranging from 7 μm to 20 μm were coated onto a AISI 316L stainless steel by electroless plating in a thermostatically controlled bath, and the composite Ni-P-BN(h) coating with an optimum BN(h) volumetric percentage of approximately 35% exhibits the best friction coefficient. Shitang Zhang et al. [16] prepared Ni/hBN coating on 1Cr18Ni9Ti stainless steel substrate by means of laser cladding on a 10 kW transverse flow continuous-wave CO_2 laser processing system. In our previous work [19], Co-based alloy/TiC/CaF_2 self-lubricating composite coatings were successfully prepared on a Cr-Zr-Cu alloy for continuous casting mold by Nd:YAG laser cladding. In general, various surface modification techniques can be employed to produce composite coatings, among which laser cladding is very effective and offers distinct advantages such as lower porosity, improved microstructure and strong metallurgical bonding.

* Corresponding author at: School of Materials Engineering, Shanghai University of Engineering Science, Shanghai 201620, China.
E-mail address: yanhua@sues.edu.cn (H. Yan).

http://dx.doi.org/10.1016/j.surfcoat.2017.06.079
Received 22 March 2017; Received in revised form 5 June 2017; Accepted 7 June 2017
0257-8972/

Please cite this article as: Yan, H., Surface & Coatings Technology (2017), http://dx.doi.org/10.1016/j.surfcoat.2017.06.079

Table 1
Characteristics of the as-received powders for laser cladding.

Powder type	Composition (wt%)	Powder size (μm)	Melting point (°C)
Ni60	Ni-16Cr-4B-4Si-0.7C	35–60	960–1040
Nano-h-BN	Purity 98.5%	~0.1	–
Nano-Ni	Purity 99.99%	0.01–0.04	–

It has been already widely accepted that developing lubricating additives with high efficiency and without pollution by using nanoparticles as lubricating additives is a new way. Unfortunately, very few data are currently available on the self-lubricating properties of laser cladding composite coatings containing nanoparticles h-BN. The synthesis of nickel based h-BN composite lubrication coatings was investigated with different laser cladding processes in this paper, and a novel method was developed for improving the material compatibility between the metal matrix and h-BN by encapsulating h-BN with nano-Ni, and controlling the reaction of nano-h-BN with other elements. And the effects of laser cladding process on composite coating morphology and properties were discussed.

2. Experimental procedure

A medium carbon steel with a composition of Fe-0.45C-0.3Si-0.6Mn (wt%) was adopted as the substrate for laser cladding treatment, the surface of which was ground to a surface finish of Ra 0.8 μm, then rinsed with ethanol followed by acetone before laser cladding. Coating materials used in the experiment were the mixture of nano-Ni/h-BN and Ni60 self-fluxing powders, as tabulated in Table 1.

Two types of powder mixtures were prepared for laser cladding treatment. The first types of Ni60 with nano-h-BN mixtures were blended by a low energy ball milling manner to ensure a uniform dispersion of the metal powder and the lubricant. Considering the physicochemical characteristics of the nano-sized lubricant h-BN, i.e., high specific surface of the nano-sized h-BN, poor wetting property of the h-BN by metal melt because of their totally different chemical structures and much lower density (2.27 $g{\cdot}cm^{-3}$) in comparison with that of the metal matrix (about 8.9 $g{\cdot}cm^{-3}$), the light h-BN particles easily float up to the top of the laser-clad coating, which results in a hard synthesis of nano-sized h-BN into the metal matrix coating during fast laser cladding process. Consequently, the nano-sized h-BN particles were clad with nano-Ni powder by high energy milling at a high mass ratio of ball to power 20:1 for 3 h to enhance the interfacial compatibility between h-BN and Ni60 matrix. Therefore, the second type of power mixtures was blended with nano-Ni-clad nano-h-BN and Ni60 alloy by low energy ball milling. Different powder mixtures for laser cladding treatment are listed in Table 2.

To fabricate Ni-based alloy self-lubricating composite coatings, 0.7 mm-thick powder mixture coatings were preplaced onto the substrate by an organic binder and then oven-dried before laser cladding. Laser cladding experiments were carried out by 400 W Nd:YAG laser and 5 kW continuous-wave CO_2 laser, respectively. The YAG laser was operated at an average power level of 370 W while pulse width, frequency, scanning velocity and laser beam diameter were fixed at 0.5 ms, 60 Hz, 120 mm s^{-1} and 3 mm respectively. The average power of CO_2 laser cladding process for different components was fixed at 1800 W and 2100 W, respectively. And scanning velocity was 200 mm s^{-1}. Large cladding surface was achieved by multi-track treatment at an overlapping ratio of 30%. Laser beam was defocused into a diameter of 6 mm.

Table 2
Mixtures of powders used for laser cladding treatment.

Mixture No.	Components (wt%)		
	Ni60	h-BN	Nano-sized Ni
1	95	5.0	–
2	90	10.0	–
3	87.5	5.0	7.5
4	75.0	10.0	15.0

The cross sections of laser-clad samples (polished to 3 μm) were characterized by scanning electron microscopy (SEM) incorporating energy dispersive X-ray analysis (EDX). The corresponding component phases of coatings were determined using X-ray diffraction with Cu-Ka radiation. Microhardness at the cross-section of the coatings was measured with Vicker microhardness testing machine (Buchler-III) under 100 g load and 10 s dwell time.

Friction coefficients of coatings were evaluated using a pin-on-ring friction tester (MMS-1G). The ring with a dimension of Ø400 mm × 30 mm was hardened ball bearing steel AISI E52100 with a hardness of HRC 60–62. The pin specimens with a dimension of 10 mm (long) × 5 mm (wide) × 20 mm (high) were fixed in a holder of the test rig. The friction coefficient of the cladding layer was evaluated by using sliding speed 2 $m{\cdot}s^{-1}$ at a constant normal load 20 N under dry friction/wear condition. The friction coefficient μ was calculated using the expression:

$$\mu = T/RP \tag{1}$$

where T is the friction moment, R the radius of the ring, and P the normal load acted on pin specimens.

3. Results and discussion

3.1. Microstructure of laser-clad coatings

The cross-section SEM photographs of laser-clad Ni-based alloy/nano-Ni encapsulated h-BN self-lubricating composite coatings are displayed in Fig. 1. On the basis of scale in the SEM photographs, the thickness of the coatings can be estimated. The thickness of the coatings by Nd:YAG laser cladding and CO_2 laser cladding was about 0.4 mm and 0.55 mm, respectively. The defect-free coatings were prepared by laser cladding using two types of lasers: a 5 kW CW CO_2 laser and a 400 W pulsed Nd:YAG laser.

Fig. 2 shows the typical microstructures at three different regions of the Nd:YAG laser-clad coatings, i.e., the upper region, the intermediate region and the bottom region. For Mixture No.1 component, many white and grey particles were distributed in the Ni-based alloy solid solution matrix, and with more near to the top surface of coating, larger grey particles were generated, but fine white particles mainly existed in the bottom regions. The compositions of both larger grey particles and fine white particles (see Fig. 1(a)) analyzed by EDX indicate that the larger grey particles and the white grains are B-rich and C-rich alloys, respectively. The component phases of the laser-clad coatings were identified by X-ray diffraction analysis, the main phases were nickel based solution γ-(Ni, Fe) with a face centered cubic (fcc) structure, and some complicated compounds, such as CrB, Ni_3B, or even possibly Cr_7C_3, and almost no h-BN phase was detected in the coating, as shown in Fig. 3. It could be interesting to note that there existed obvious differences in the cross-sectional microstructures of the coatings along the depth direction. It is because part of h-BN was floating on the top surface of the coating after laser cladding, owing to its softness and smaller density, leaving behind a lot of irregular pores near the top surface and rapid directional solidification microstructure was formed perpendicular to the interface showing columnar cellular/dendrite structures [18].

Fig. 4 shows the typical microstructures at three different regions of the CO_2 laser cladding coatings. Many dendritic structures were found in the intermediate and bottom regions, and nearly no dendrites at the top region of coating. For Ni60-5 wt% h-BN coating, dendrites in the bottom region grew perpendicularly to the interface between coating

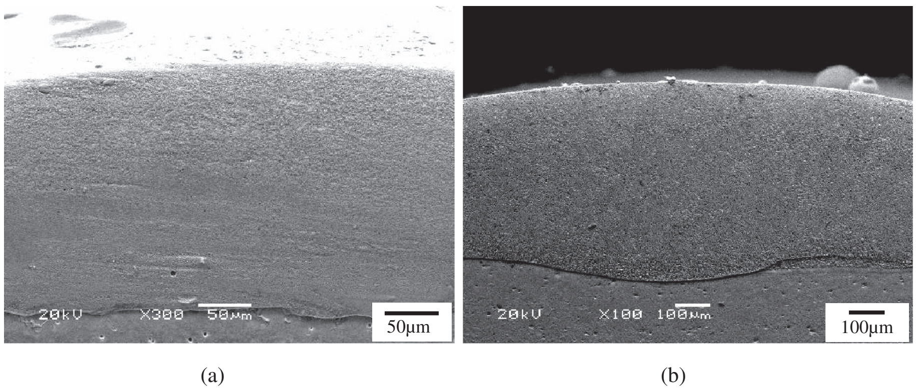

Fig. 1. Cross-section morphology of laser-clad Ni-based alloy/nano-Ni encapsulated h-BN self-lubricating composite coatings: (a) Nd:YAG laser-clad and (b) CO_2 laser-clad.

and substrate, and these dendrites grew up to coarse structure in the intermediate region. In addition, a few white particles were imbedded in the intergranular regions, which were restricted to be coarse precipitates. With the increasing of h-BN content, intermetallic compound of borides further grew into dendrite crystals, and some secondary dendrites formed vertically along the primary dendrite arms, as shown in Fig. 4(f). Which maybe attribute to higher laser energy, laser molten pool maintained at a higher temperature, more fine grains nucleated on primary dendrites, and gradually grew up into secondary dendrites. Besides, fine white intermetallics could be found on the top of coating, but no dendrites in this region. The findings are in line with the results of researches by Niu [17] and Yan [18].

Fig. 5 shows the microstructure of Ni-based nano-Ni encapsulated h-BN coating with YAG laser cladding process. In which some micron-sized grey particles and nano/submicron sized white particles are distributed on the Ni-based alloy dendrite. The micron-sized grey particles are Cr_7C_3 because of its much rich Cr content while the nano/submicron sized white particles are nano-Ni encapsulated h-BN or intermetallic compound of borides because of its much rich B and nickel content revealed by SEM and EDX analysis (listed in Table 3).

For the laser-clad Ni60-BN coatings (seen in Fig. 3), the main phase

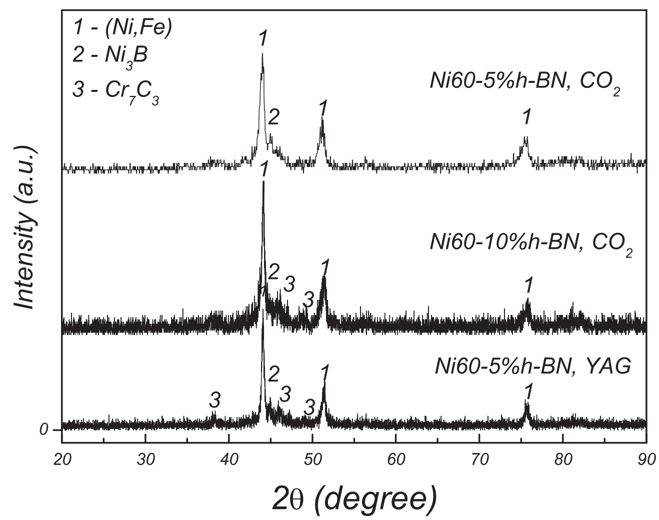

Fig. 3. XRD spectra of Ni60-hBN coatings with different laser cladding processing.

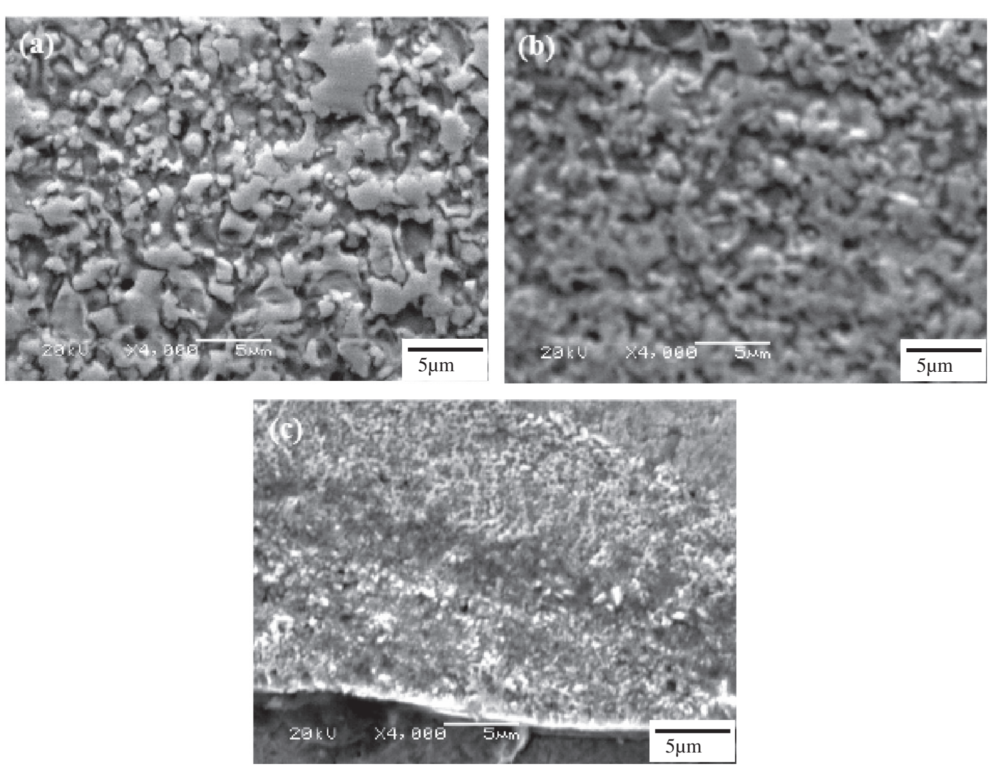

Fig. 2. Typical microstructure at different regions of the Nd:YAG laser-clad Ni60-5 wt% hBN coating: (a) upper region, (b) intermediate region, (c) bottom region.

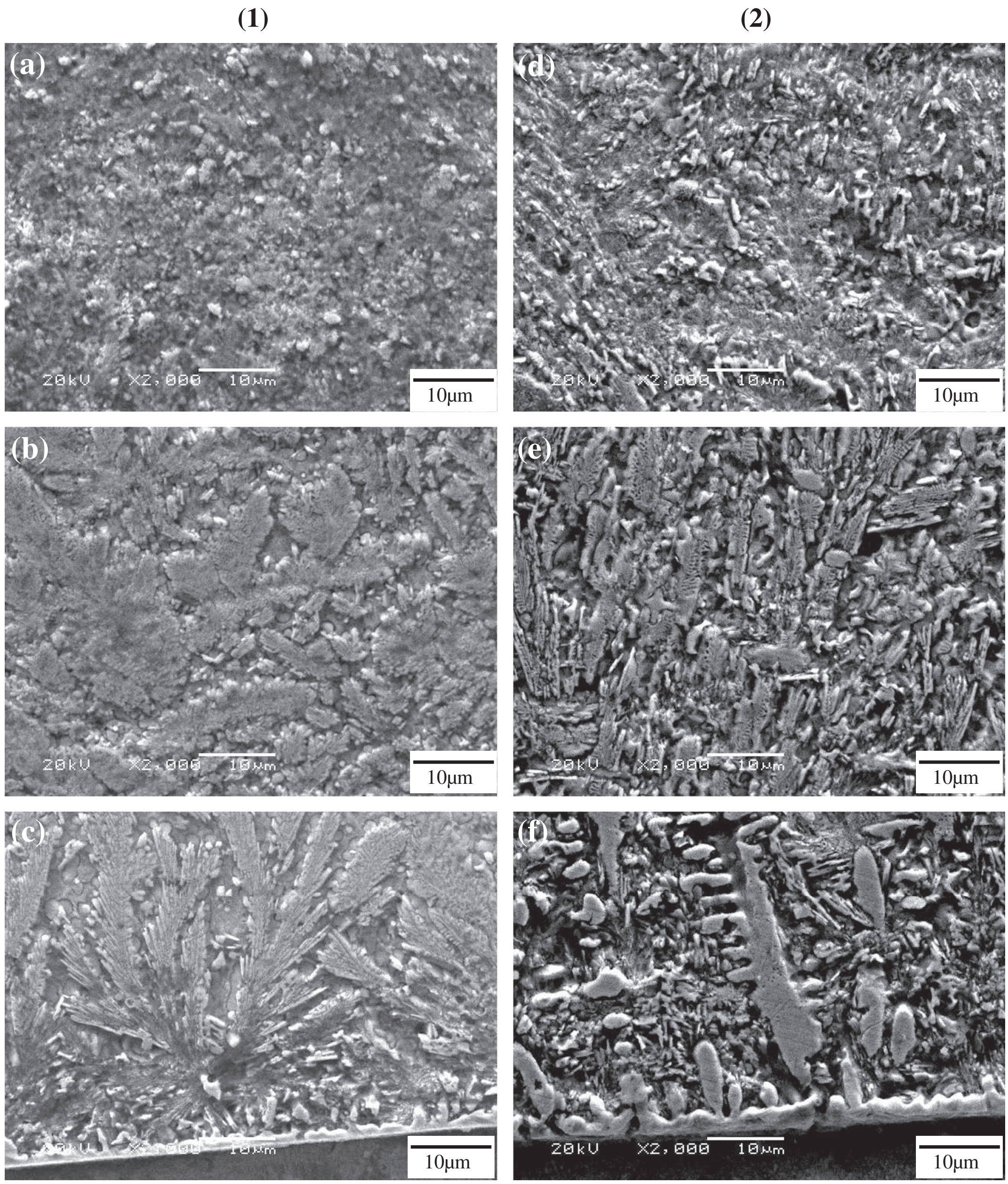

Fig. 4. Typical microstructure at different regions of the CO_2 laser-clad coating: (1) microstructure of the laser-clad Ni60-5 wt% hBN coating at 1800 W (a) upper region, (b) intermediate region, (c) bottom region; (2) microstructure of the laser-clad Ni60-10 wt% hBN coating at 2100 W (d) upper region, (e) intermediate region, (f) bottom region.

for all laser-clad coatings is Ni-based solid solution with a fcc structure and no h-BN diffraction peaks are found in the XRD spectra. While apparent h-BN diffraction peaks are observed for the laser-clad Ni60-hBN coatings at both BN content of 5 wt% and 10 wt%(seen in Fig. 6). This supports that nano-sized h-BN can be effectively added into the laser-clad coatings after high-energy ball milling of nano-sized Ni onto h-BN surface.

3.2. Microhardness and tribological behaviors

Fig. 7 shows the microhardness of Ni-based h-BN composite coating. From the top surface of coatings to interface between coating/substrate, the hardness of coatings presented a descending tendency, and reached the minimum values in the heat affected zones, which conformed to the distributions of phases in coatings. For h-BN and nano-nickel are soft materials in coatings, the hardness of Ni60-10wt%BN (nano-Ni-encapsulated) coating was lower than that of others, but the decreasing trend of which was smooth. This indicated that h-BN particles were prevented from floating up to the upper regions of coating when encapsulated with nano-nickel. On the opposition, h-BN non-encapsulated with nano-nickel mostly rose up to the upper zones of coatings, and took chemical reaction with nickel, chrome and other elements in the melting laser pool, and these borides with higher hardness enhanced the microhardness of the top layer. In CO_2 laser cladding processing, higher power laser and higher energy density promoted a higher temperature molten pool, which was beneficial to the floating of h-BN and generation of borides and carbides in the sequent solidification stage.

Fig. 8 presents the friction coefficients of two typical laser-clad coatings. The friction coefficient of the CO_2 laser-clad Ni60-hBN coating increases from 0.5 to 0.6 gradually with an increase in sampling time. In YAG laser cladding processing, the addition of nano-Ni-encapsulated nano-h-BN into the laser-clad Ni60 coating dramatically decreases the friction coefficient to about 0.36. This indicates that the frictional performance was significantly improved by effective addition of nano-

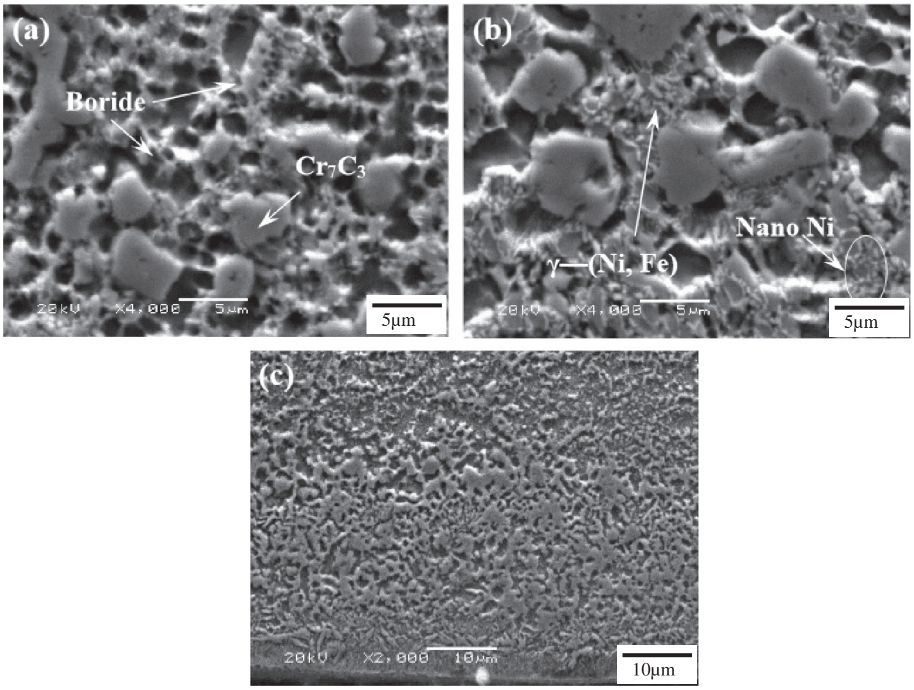

Fig. 5. Microstructure of the laser-clad Ni60-10 wt% hBN (nano-Ni-encapsulated) coating: (a) upper region, (b) intermediate region, (c) bottom region.

Table 3
Compositional analysis of the laser-clad Ni60-BN (nano-Ni-clad) coating.

Area	Composition (wt%)				
	B	Si	Cr	Fe	Ni
White particle	15.61	03.67	04.98	14.96	60.78
Grey particle	0.0	00.60	88.89	07.67	02.83

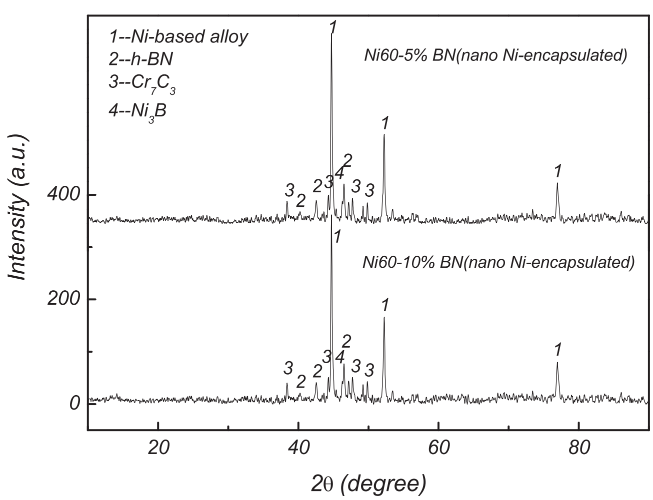

Fig. 6. XRD spectra of Ni60-nano-Ni encapsulated hBN laser-clad coatings.

Ni-clad BN into Ni60 matrix.

4. Conclusions

1) For laser cladding of the Ni60-hBN coating, the high-energy ball milling of nano-Ni onto nano-h-BN significantly improved the interfacial compatibility between h-BN and Ni60 matrix, and Ni-based alloy matrix nano-h-BN composite coatings were successfully synthesized.
2) The main phases in laser-clad coating are composed of hard precipitates CrB, Ni_3B, Cr_7C_3 and nickel based solid solution (γ), which are mostly distributed in the upper layer of laser cladding zone, and greatly promote the microhardness of the coatings.
3) Compared with CO_2 laser cladding process, Nd:YAG laser molten pool suppressed h-BN floating up to upper regions of coating for lower temperature and quick solidification.
4) The friction coefficient of Nd:YAG laser-clad Ni60-10 wt% hBN (nano-Ni encapsulated) coating was reduced significantly to about 0.36, which was lower than that of the laser-clad Ni60/h-BN coating without nano-Ni-clad.

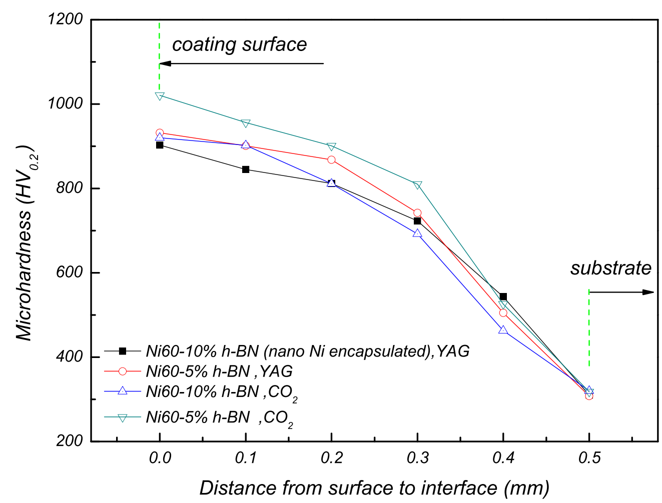

Fig. 7. Microhardness of Ni-based h-BN composite coating.

Acknowledgements

The authors wish to acknowledge the financial support of National Natural Science Foundation of China (51405288, 51605276, 51571214) and Shanghai Science and Technology Committee Innovation Grant (17JC1400600 , 17JC1400601).

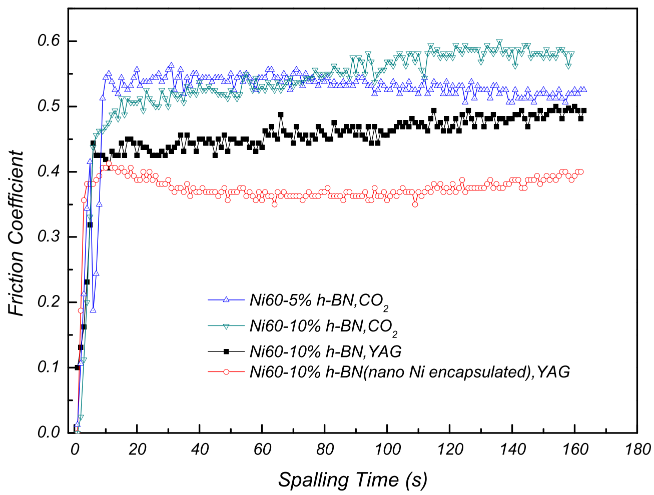

Fig. 8. Friction coefficient comparison of the laser-clad Ni60-hBN and Ni60-10 wt% hBN (nano-Ni-encapsulated) coatings.

References

[1] A. Yakovlev, Ph. Bertrand, I. Smurov, Thin Solid Films 453-454 (2004) 133–138.

[2] C. Donnet, A. Erdemir, Surf. Coat. Technol. 180-181 (2004) 76–84.

[3] Y. Wang, Z. Liu, Wear 265 (2008) 1720–1726.

[4] Y.X. Wu, F.X. Wang, Y.Q. Cheng, N.P. Chen, Wear 205 (1997) 64–70.

[5] T. Kondo, K. Shindo, Y. Sakurai, J. Alloys Compd. 386 (2005) 202–206.

[6] J.H. Ouyang, S. Sasaki, K. Umeda, Surf. Coat. Technol. 137 (2001) 21–30.

[7] P. Skarvelis, G.D. Papadimitriou, Tribol. Int. 42 (2009) 1765–1770.

[8] W.S. Cho, M.W. Cho, J.H. Lee, Z.A. Munir, Mater. Sci. Eng. A 418 (2006) 61–67.

[9] L. Avril, B. Courant, J.J. Hantzpergue, Wear 260 (2006) 351–360.

[10] Y. Tsunekawa, I. Ozdemir, M. Okumiya, J. Therm. Spray Technol. 2 (2006) 239–245.

[11] I. Ozdemir, Prakt. Metallogr. PR. M. 8 (2007) 355–371.

[12] C. Tekmen, I. Ozdemir, G. Fritsche, Y. Tsunekawa, Surf. Coat. Technol. 203 (2009) 2046–2051.

[13] X.F. Zhang, L. Zhang, Z.Y. Huang, Adv. Tribol. (2015) 621278-6.

[14] O.A. Leon, M.H. Staia, H.E. Hintermann, Surf. Coat. Technol. 108-109 (1998) 461–465.

[15] O.A. Leon, M.H. Staia, H.E. Hintermann, Surf. Coat. Technol. 200 (2005) 1825–1829.

[16] S.T. Zhang, J.S. Zhou, B.G. Guo, H.D. Zhou, Y.P. Pu, J.M. Chen, Mater. Sci. Eng. A 491 (2008) 47–54.

[17] W. Niu, R.L. Sun, Y.W. Lei, Adv. Mater. Res. 154-155 (2011) 609–612.

[18] H. Yan, A.H. Wang, X.L. Zhang, Z.W. Huang, W.Y. Wang, J.P. Xie, Mater. Sci. Technol. 26 (2010) 461–468.

[19] H. Yan, J. Zhang, P.L. Zhang, Z.S. Yu, C.G. Li, P.Q. Xu, Y.L. Lu, Surf. Coat. Technol. 232 (2013) 362–369.